STOCHASTIC TEXTURE IMAGE RETRIEVAL AND SIMILARITY MATCHING

JUNG C.R.[1], SCHARCANSKI J.[2]

[1,2] UFRGS–Universidade Federal do Rio Grande do Sul
Instituto de Informática
Av. Bento Gonçalves, 9500. Porto Alegre, RS, Brasil 91501-970
[1] jung@inf.ufrgs.br
[2] jacobs@inf.ufrgs.br

[1] UNISINOS - Universidade do Vale do Rio dos Sinos
Departamento de Matemática
Av. UNISINOS, 950. São Leopoldo, RS, Brasil, 93022-000
crjung@exatas.unisinos.br

Abstract. Stochastic texture images representing various foil materials (like polymer sheets, nonwoven textiles and paper) provide important information about these materials, and are very utilized in industry. Often, it is difficult to objectively measure the similarity among those images, or to discriminate images of different types of materials. This work proposes a new multi-resolution method for texture image discrimination and similarity matching. The wavelet transform is used to represent the images in multiple resolutions, and to describe them in terms of their orientation and graylevel distributions. It is also proposed a multi-resolution similarity measure based on this representation. Finally, some experiments illustrate the performance of our method, and some conclusions are presented.

Keywords: Quality Control, Texture Image Representation, Similarity Matching and Pattern Recognition, Multi-Resolution Image Analysis, Image Databases.

1 Introduction

Texture image analysis and discrimination often arise in quality control of foil-like manufactured materials, like paper and non-woven textiles. In general, these images contain important information, represented by a composition of periodic and stochastic features at various scales, resulting from local clumping and aligning of constituent matter with varying degree of regularity. Such images are often stored in large digital catalogs, and many times we face the difficult problem of retrieving images that are similar to a given example, as well as some product or process information associated to the retrieved images (e.g. finding products in a catalog that have properties similar to a provided paper sample). In this context, it is important to determine a set of parameters for texture representation and discrimination, as well as a similarity measure, that could be used to retrieve images similar to a given example from a database (i.e. a digital image catalog).

A study conducted by Rao and Lohse [1] has indicated that three dimensions are important in natural texture discrimination, namely, "repetitiveness", "directionality", and "granularity and complexity". A retrieval system based on these three dimensions should reproduce human perceptual saliencies. Liu and Picard [2] proposed a retrieval system based on the Wold decomposition of textures, that incorporates the three features suggested by Rao and Lohse. However, it is not clear how such features extend to similarity matching of stochastic textures, such as those found in paper and non-woven textile samples.

Texture anisotropy in multiple resolutions may provide an estimate of the "directionality" dimension proposed by Rao and Lohse. A method was suggested by Scharcanski and Dodson [3] for anisotropy measurement in stochastic textures, which uses local gradient distributions and local dominant orientations. Good results were obtained with this approach, but its performance in multiple scales is not satisfactory. The same authors [4] proposed to calculate anisotropy in stochastic textures using the correlation of local gradients within a given neighborhood. However, this method is also limited in terms of multi-scale analysis.

In this work, the image grayscale distribution and texture anisotropy are measured at different resolutions, using the wavelet transform. Based on these features, a representation in multiple resolutions is assembled, and we show that stochastic texture discrimination and similarity matching may be achieved using such a representation. The next sections describe a technique to detect local gradients in

0-7695-0878-2/00 $10.00 © 2000 IEEE

multiple resolutions using wavelets, and our approach to stochastic texture representation. Finally, we present some experimental results and conclusions.

2 Measuring Local Graylevel Variability in Multiple Resolutions

We measure local graylevel variability at different resolutions based on local gradients. In order to estimate the local gradients in multiple resolutions, we utilize the redundant two-dimensional wavelet transform proposed in [5]. Below, we briefly describe the wavelet transform in two dimensions, and how to detect local gradients in a texture image using wavelets.

2.1 Wavelet Transform in Two Dimensions

In this work, the 2-D wavelet decomposition uses only two detail images (horizontal and vertical details) [5], instead of the already conventional approach where three detail images (horizontal, vertical and diagonal details) are used [6]. This two-dimensional wavelet transform requires two wavelets, namely, $\psi^1(x,y)$ and $\psi^2(x,y)$. At a particular scale s we have:

$$\psi_s^i(x,y) = \frac{1}{s^2}\psi^i(\frac{x}{s},\frac{y}{s}),\ i=1,2. \tag{1}$$

The dyadic wavelet transform $f(x,y)$, at a scale $s = 2^j$ has two components given by:

$$W_{2^j}^i f(x,y) = f * \psi_{2^j}^i(x,y),\ i=1,2. \tag{2}$$

Therefore, the multi-resolution wavelet coefficients are:

$$\mathbf{W}_{2^j} f(x,y) = \left(W_{2^j}^1 f(x,y), W_{2^j}^2 f(x,y)\right). \tag{3}$$

The original signal $f(x,y)$ is then represented by the two dimensional wavelet transform, in terms of the two dual wavelets $\xi^1(x,y)$ and $\xi^2(x,y)$:

$$\begin{aligned} f(x,y) &= \sum_j ((W_{2^j}^1 f(x,y) * \xi_{2^j}^1(x,y) + \\ &\quad + W_{2^j}^2 f(x,y) * \xi_{2^j}^2(x,y)) \end{aligned} \tag{4}$$

In order to build a multi-scale representation, we need a scaling function $\phi(x,y)$, whose integral over the plane equals "1", and tends to "0" at infinity [5]. Thus, $\phi(x,y)$ is a smoothing function, and its component at a scale 2^j is:

$$S_{2^j} f(x,y) = f * \phi_{2^j}(x,y). \tag{5}$$

We may interpret the component $S_{2^J} f(x,y)$ as a smoothed version of $f(x,y)$, and the components $\mathbf{W}_{2^j} f(x,y)$, for $j = 1,...,J$, as the image details lost by smoothing going from $S_{2^0} f(x,y)$ to $S_{2^J} f(x,y)$. Further details may be found in [5] and [6].

2.1.1 Local Gradients in Multiple Resolutions

Now, it is necessary to find a wavelet basis such that its components $\mathbf{W}_{2^j} f(x,y)$ are related to the local gradients of the image at the scale 2^{j-1}. A smoothing function $\varsigma(x,y)$ is selected such that its integral over the plane $\mathbb{R}^2$ is equal to "1", and it converges to "0" at infinity. We then define:

$$\psi^1(x,y) = \frac{\partial}{\partial x}\varsigma(x,y) \text{ and } \psi^2(x,y) = \frac{\partial}{\partial y}\varsigma(x,y). \tag{6}$$

Note that the wavelet coefficient $\mathbf{W}_s f(x,y)$ can be written as:

$$\begin{aligned} \mathbf{W}_s f(x,y) &= \begin{pmatrix} W_s^1 f(x,y) \\ W_s^2 f(x,y) \end{pmatrix} = \\ &= s\begin{pmatrix} \frac{\partial}{\partial x}(f * \varsigma_s)(x,y) \\ \frac{\partial}{\partial y}(f * \varsigma_s)(x,y) \end{pmatrix} = \\ &= s\nabla(f * \varsigma_s)(x,y), \end{aligned} \tag{7}$$

which in fact corresponds to the gradient of the smoothed version of f at the scale s. Thus, the coefficient $\mathbf{W}_s f(x,y)$ can be used as an estimate for the gradient of the image at the scale s. Using dyadic scales ($s = 2^j$), the gradient magnitude is given by:

$$\|\mathbf{W}_{2^j} f(x,y)\| = \sqrt{W_{2^j}^1 f(x,y)^2 + W_{2^j}^2 f(x,y)^2}, \tag{8}$$

and the gradient orientation can be calculated from:

$$\theta_{2^j}(x,y) = \arctan\left(\frac{W_{2^j}^2 f(x,y)}{W_{2^j}^1 f(x,y)}\right). \tag{9}$$

Equations (8) and (9) are used to obtain the magnitude and orientation of the gradients in multiple resolutions. Because we are interested in digital images $f[n,m]$, we use a discrete version of the wavelet transform [5].

3 Texture Representation in Multiple Resolutions

3.1 Texture Directionality Representation

We use the distribution of angles $\theta(x,y)$ over all locations (x,y), at different resolutions, to represent structural anisotropy [4]. When all angles θ are equally probable, the sample is isotropic.

Scharcanski and Dodson [3] used a threshold to suppress the influence of noise in the angular distribution. However, usually gradient magnitudes associated to noise are smaller than magnitudes related to texture image structures. Therefore, we use the edge magnitude as a "weight", and obtain a modified angular distribution in such a way that a threshold is no longer needed, and noise influence is minimized, as it is explained next.

In order to estimate the angular distribution, initially the interval $[0, 2\pi)$ is divided in N equally spaced subintervals, whose centers are denoted by $\theta_i = \frac{2\pi i}{N}$, $i = 0, 1, ..., N-$

1. The angles $\theta_{2^j}(x,y)$ are quantized to the closest θ_i value. Let us denote by $k(\theta_i)$ the sum of the gradient magnitudes along the quantized direction θ_i. The resulting polar plot of $\theta_i \times k(\theta_i)$ is typically elliptic for anisotropic samples, and tends to be circular for isotropic samples. Figure 1 shows the polar plots of two different texture images, appearing in Figure 3 (i.e. *md1j44a1* and *pxxe50c1*). Texture *md1j44a1* is isotropic, while texture *pxxe50c1* is anisotropic. Both polar plots were calculated at the resolution 2^2.

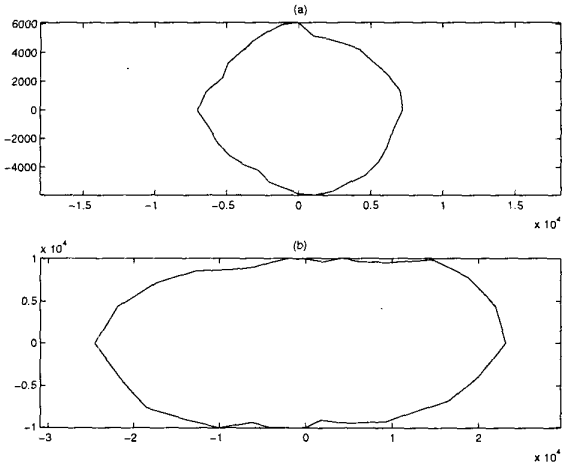

Figure 1: Polar plots: (a) Texture *md1j44a1*. (b) Texture *pxxe50c1*.

The angular distribution determines two orthogonal axes of extremal variance, that coincide with the directions of the eigenvectors $\mathbf{v}_{\max}$ and $\mathbf{v}_{\min}$ of the covariance matrix [3]. In order to estimate the covariance matrix, we calculate:

$$\begin{matrix} \mathbf{p}_x(i) = k(\theta_i)\cos(\theta_i) \\ \mathbf{p}_y(i) = k(\theta_i)\,\mathrm{sen}(\theta_i) \end{matrix} \quad , i = 0, 1, ..., N-1. \qquad (10)$$

Let us denote the means of the vectors $\mathbf{p}_x$ and $\mathbf{p}_y$ by μ_x^θ and μ_y^θ, respectively. The covariance matrix is then calculated by:

$$\mathbf{C}(i,j) = \frac{1}{(N-1)^2} \sum_{i=0}^{N-1} \sum_{j=0}^{N-1} \left(\mathbf{p}_x(i) - \mu_x^\theta\right)\left(\mathbf{p}_y(j) - \mu_y^\theta\right). \qquad (11)$$

Please, notice that the eigenvectors $\mathbf{v}_{\max}$ and $\mathbf{v}_{\min}$ are obtained from (11), as well as the corresponding eigenvalues $\lambda_{\max}$ and $\lambda_{\min}$. The eigenvalues $\lambda_{\max}$ e $\lambda_{\min}$ define the semi-axes of an ellipse aligned with the directions of the eigenvectors. The eccentricity e of this ellipse is given by the ratio of the eigenvalues:

$$e = \frac{\lambda_{\max}}{\lambda_{\min}}. \qquad (12)$$

The calculated eccentricity e provides a measure for the texture anisotropy. It should be noticed that the eccentricity can be calculated at different resolutions, since equation (9) provides angular information at each scale 2^j. Please, notice that the main orientation of the texture at each scale is given by the direction of $\mathbf{v}_{\max}$.

3.2 Texture Graylevel Representation

The texture graylevel distribution estimated at each resolution also contains important information. At each scale 2^j, the distribution is represented by the graylevel histogram of the corresponding image $S_{2^j}f(x,y)$ (i.e. a smoothed version of the texture image at resolution 2^j). This histogram is represented by a vector $\mathbf{g}_j$, with length N_g.

Typically, samples of similar textures also have similar graylevel histograms, and we use this information for texture discrimination and similarity matching. Please, notice that information provided by the angular distribution is orthogonal to that provided by the graylevel distribution. In this work, both are combined in a texture similarity measure, as it will be discussed later.

Figure 2 shows the histograms of two different texture images appearing in Figure 3, namely, *md1j44a1* and *pxxe50c1*. It can be noticed that sample *md1j44a1* has smaller mean graylevel than texture *pxxe50c1*, since the histogram peak is closer to the origin.

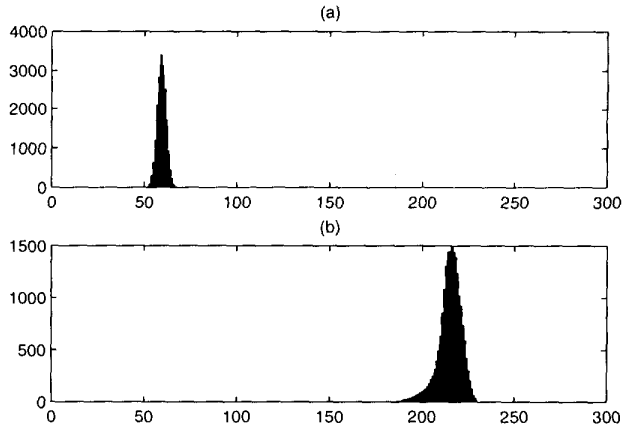

Figure 2: Graylevel histograms: (a) Texture *md1j44a1*. (b) Texture *pxxe50c1*.

3.3 Texture Similarity Matching

In order to measure the similarity among texture images, the angular and graylevel information are combined into a multi-resolution similarity measure. Our similarity matching procedure is described next.

For the texture example provided by the user, the angular and graylevel histograms, denoted respectively by $\mathbf{k}_j^{\text{sample}}$ and $\mathbf{g}_j^{\text{sample}}$, are calculated at each resolution 2^j. The angular histogram $\mathbf{k}_j^{\text{test}}$ and graylevel histogram $\mathbf{g}_j^{\text{test}}$ corresponding to each texture image in the database, at each resolution 2^j, are compared to those obtained from the texture example.

The angular dissimilarity between the example and the database test image is measured by the Euclidean distance d_j^{ang} between vectors $\mathbf{k}_j^{\text{sample}}$ and $\mathbf{k}_j^{\text{test}}$, which is calculated by:

$$d_j^{\text{ang}} = \left\| \mathbf{k}_j^{\text{sample}} - \mathbf{k}_j^{\text{test}} \right\|. \tag{13}$$

In a similar way, the Euclidean distance d_j^{dens} between vectors $\mathbf{g}_j^{\text{sample}}$ and $\mathbf{g}_j^{\text{test}}$ measures the graylevel dissimilarity, and it is calculated by:

$$d_j^{\text{dens}} = \left\| \mathbf{g}_j^{\text{sample}} - \mathbf{g}_j^{\text{test}} \right\|. \tag{14}$$

Given the distances d_j^{ang} and d_j^{dens}, a texture similarity measure is obtained at the resolution 2^j, as described next. Considering that these two distances are associated to orthogonal feature space dimensions, they are combined in a unified distance measure. It should be noticed that vectors $\mathbf{k}_j$ and $\mathbf{g}_j$ may have different lengths. To compensate for this difference, a normalization factor is utilized. The distance d_j^{dens} is multiplied by $\sqrt{\frac{N_g}{N}}$, where N and N_g represent, respectively, the lengths of $\mathbf{k}_j$ and $\mathbf{g}_j$. The distances d_j^{ang} and d_j^{dens} are then combined using the Euclidean norm, as follows:

$$d_j = \sqrt{(d_j^{\text{ang}})^2 + (d_j^{\text{dens}})^2}. \tag{15}$$

To take into account different resolutions 2^j, the distances d_j are combined to obtain the multi-resolution distance measure:

$$d = \sum_{j=1}^{J} d_j, \tag{16}$$

where J is the number of scales used in the wavelet transform. To complete this similarity matching procedure, all samples in the database are organized in decreasing order with respect to the multiresolution distance d, and a selection of the M most similar are shown to the user.

4 Experimental Results

To illustrate the performance of our method, we used β-radiographic images of paper samples, all with resolution of 280 × 280 pixels, obtained from [7]. For each of these textures, nine sub-images (140 × 140 pixels) were obtained (with superposition). Samples of nine different types of paper were used in our experiments, and a total of 81 images were stored in the database. Figure 3 shows samples of the nine different samples utilized in our experiments. Two dyadic scales were used (2^j, for $j = 1, 2$). The vectors $\mathbf{g}_j$ and $\mathbf{k}_j$ have, respectively, lengths of 256 and 32.

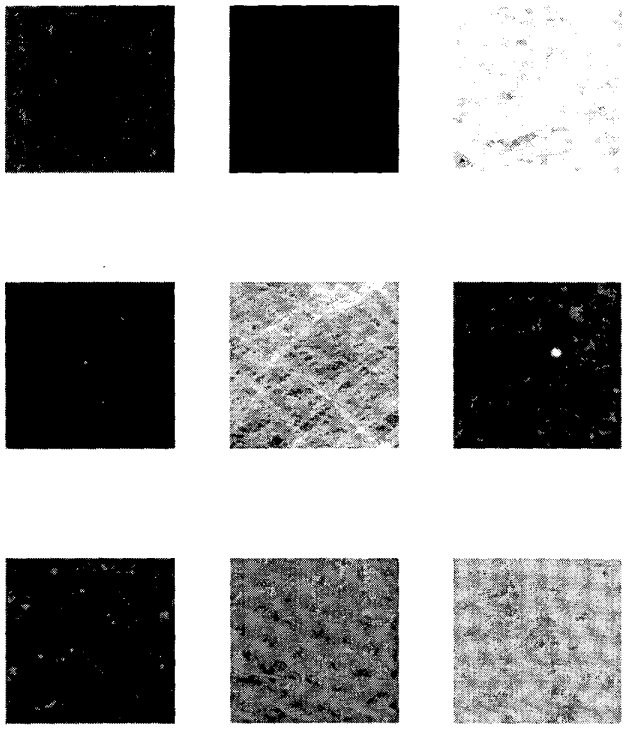

Figure 3: The nine textures used in the experiments. From left to right, top to bottom: *md1j44a1, pxxe46b1, pxxe50c1, axxs24a5, gxo5adg1, hsma33b3, rshm36b1, msym53a2, kxa765c2.*

The performance of the algorithm proposed in the previous section is illustrated in Figure 4. The top image is a sample obtained from texture *pxxe50c1*, with resolution of 181 × 171 pixels. Please, notice that this sample has a different size than the images in the database, showing that this experiment represents a more general case. The other textures shown in Figure 4[1], from top to bottom, left to right, are the textures retrieved from the database, in decreasing order of similarity. The first nine texture retrieved are precisely the nine representative samples of the paper sample *pxxe50c1* previously stored in the database.

[1]Some of the images in this Figure had their colormaps altered, for better visualization purposes.

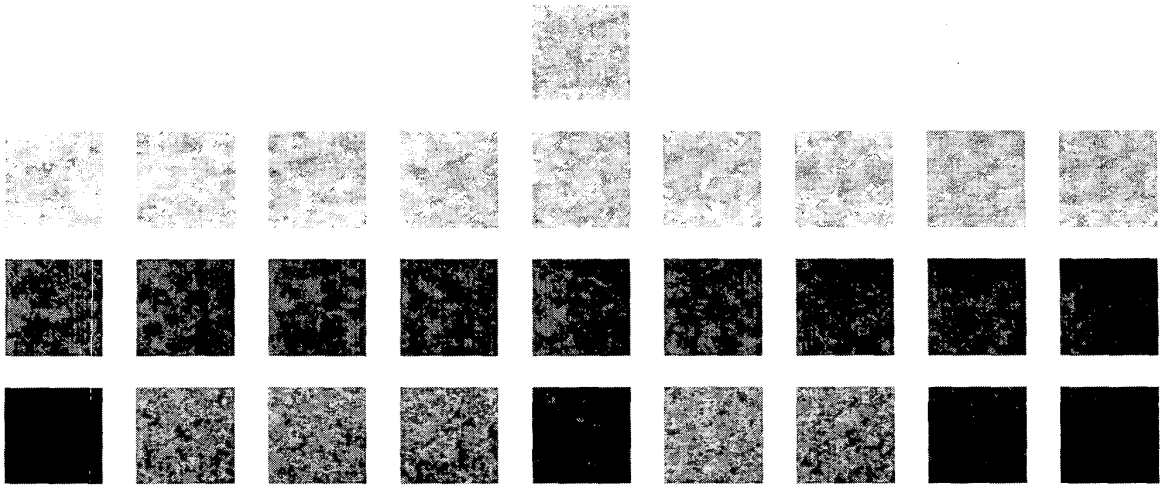

Figure 4: Results of the first similarity matching experiment. First row: sample of the texture *pxxe50c1*. Following rows: results shown in decreasing order of similarity, from left to right, top to bottom.

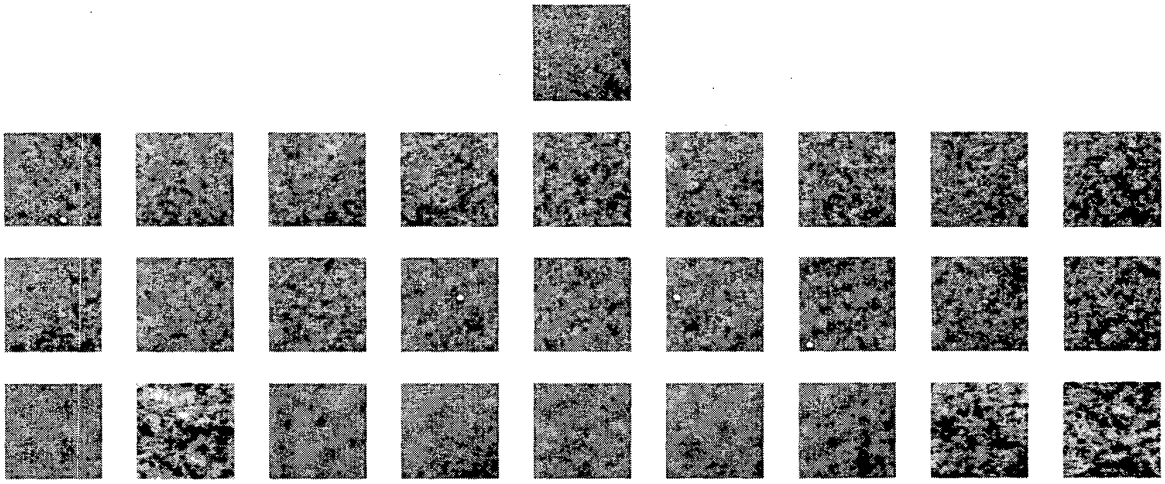

Figure 5: Results of the second similarity matching experiment. First row: sample of the texture *hsma33b1*. Following rows: results shown in decreasing order of similarity, from left to right, top to bottom.

Multiresolution Distances (*pxxe50c1*)			
d_1^{dens}	d_2^{dens}	d_1^{ang}	d_2^{ang}
2.09	1.68	0.60	1.32
1.70	1.54	1.46	2.69
2.43	1.89	1.32	2.46
2.72	2.25	1.02	1.96
2.36	2.14	1.14	2.48
1.03	1.91	2.04	3.39
1.39	2.24	2.85	4.86
1.87	2.06	2.72	4.86
1.61	1.95	3.71	6.70
16.06	16.90	3.98	6.42
16.12	16.99	4.10	6.59
16.05	16.87	4.30	7.04
16.08	16.94	4.29	6.88
16.76	17.54	2.74	4.70
16.28	17.22	4.09	6.40
16.37	17.41	3.81	6.13
16.37	17.37	3.87	6.24
16.09	16.96	4.63	7.68

Table 1: Density and anisotropy distances (levels 2^1 and 2^2) from the sample of the texture *pxxe50c1* and the images retrieved from the database, in decreasing order of similarity.

Multiresolution Distances (*hsma33b1*)			
d_1^{dens}	d_2^{dens}	d_1^{ang}	d_2^{ang}
1.02	1.59	1.05	2.00
1.20	1.99	1.32	2.47
1.50	2.30	1.05	2.11
2.93	3.71	3.32	5.32
4.76	6.03	1.04	2.10
3.02	4.08	3.63	5.78
2.47	2.87	4.19	6.76
5.04	6.48	1.64	2.90
2.80	3.64	4.39	7.01
5.69	7.38	1.10	1.99
4.56	5.40	3.70	5.72
5.92	7.56	1.42	2.59
6.00	7.75	1.36	2.45
6.98	9.16	1.17	2.02
6.43	8.15	3.15	5.00
5.86	7.56	4.81	7.82
6.53	8.56	4.86	7.75
8.57	10.75	2.73	4.34

Table 2: Density and anisotropy distances (levels 2^1 and 2^2) from the sample of the texture *hsma33b1* and the images retrieved from the database, in decreasing order of similarity.

Table 1 shows the graylevel and anisotropy distances for the images shown in Figure 4. From top to bottom, the graylevel and anisotropy distances (levels 2^1 and 2^2) from the user provided sample (obtained from texture *pxxe50c1*) and the first eighteen images retrieved from the database are shown. These results show that indeed the first matches are closer to the sample provided by the user.

Figure 5[2] shows a similar result, for a sample of the texture *hsma33b1* with resolution of 220 × 220 pixels. It should be noticed that this texture is not represented in our texture image database. Even in this case, our method shows to be robust, and retrieves textures similar to the given example.

Table 2 shows the graylevel and anisotropy distances for the images shown in Figure 5. From top to bottom, the graylevel and anisotropy distances (levels 2^1 and 2^2) from the user provided sample (obtained from texture *hsma33b1*) and the first eighteen images retrieved from the database are shown.

The multi-resolution anisotropy measure proposed in this work can also be used as an orientation measure for natural textures, as shown in Figure 6. First line shows two samples of the *straw* texture, from the Brodatz Album [8]. The second image is rotated 30° with respect to the first one. In the following rows, the respective polar plots are presented, at the resolutions $2^1, 2^2$ e 2^3. The major semi-axes of the ellipses indicate the main orientation of the textures. It can be noticed that the proposed method is consistent across different scales.

[2] Some of the images in this Figure had their colormaps altered, for better visualization purposes.

5 Concluding Remarks

A new method for the multi-resolution representation of stochastic texture images, such as paper and non-woven textiles, was presented. In the proposed approach, a texture is decomposed into its multiple resolution components, using the wavelet transform. At each resolution, two features were utilized to represent the texture, namely, the sample anisotropy that describes the texture directionality, and the sample graylevel histogram that describes the texture graylevel distribution. Also, based on these features, a multiresolution similarity measure was proposed.

The obtained experimental results indicate that stochastic texture similarity matching can be achieved using our approach. Also, the eccentricity obtained from equation (12) may be used as a measure for the "directionality" dimension proposed in [1].

Our future work will concentrate on improving similarity matching using statistical information, and test the

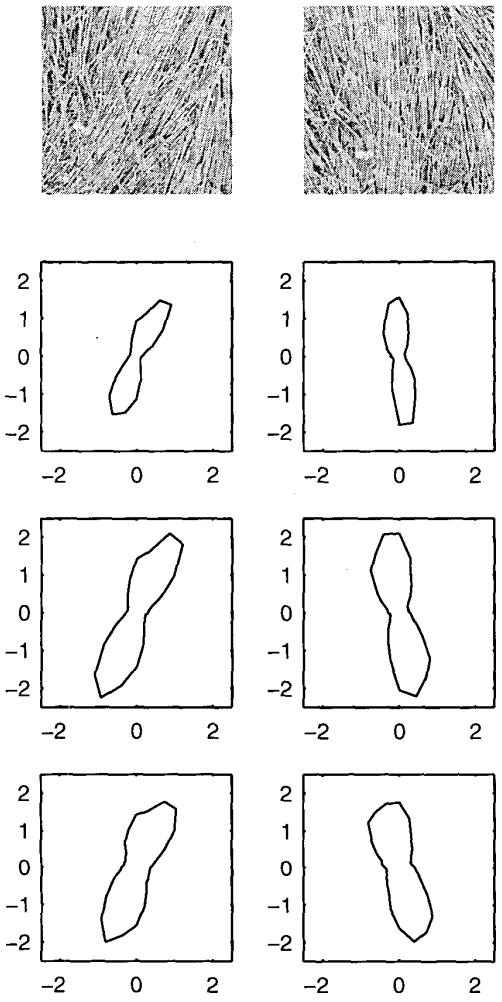

Figure 6: Orientation measurements in multiple scales. Top row: samples of the *straw* texture, from the Brodatz Album. Other rows: respective polar plots, at dyadic scales $2^1, 2^2$ and 2^3.

performance of our method in a large image database.

References

[1] A. R. Rao and G. L. Lohse, "Towards a texture naming system: Identifying relevants dimensions of texture," in *Proc. IEEE Conf. Visualization*, (San Jose, CA), pp. 220–227, October 1993.

[2] F. Liu and R. W. Picard, "Periodicity, directionality, and randomness: Wold features for image modeling and retrieval," *IEEE Trans. on PAMI*, vol. 18, pp. 722–733, July 1996.

[3] J. Scharcanski and C. T. J. Dodson, "Texture analysis for estimating spatial variability and anisotropy in planar stochastic structures," *Optical Engineering*, vol. 35, pp. 2302–2309, August 1996.

[4] J. Scharcanski and C. T. J. Dodson, "Local spatial anisotropy and its variability," *Journal of Pulp and Paper Science*, vol. 25, pp. 393–397, November 1999.

[5] S. G. Mallat and S. Zhong, "Characterization of signals from multiscale edges," *IEEE Trans. on PAMI*, vol. 14, no. 7, pp. 710–732, 1992.

[6] S. G. Mallat, "A theory for multiresolution signal decomposition: The wavelet representation," *IEEE Trans. on PAMI*, vol. 2, no. 7, pp. 674–693, 1989.

[7] C. T. J. Dodson and R. R. Singh, *Paper Stochastic Structure Analysis - Archive 2* (CD-ROM), Univ. of Toronto, Media Center, Toronto, CA. 1995.

[8] P. Brodatz, *Textures: A Photographic Album for Artists and Designers*. New York: Dover, 1966.